4E4-2

Study of Two Bands Characteristics of Mushroom-Like EBG Structures

#Long Li [1], Qiang Chen [1], Qiaowei Yuan [1], Kunio Sawaya [1], and Changhong Liang [2]
[1] Department of Electrical and Communication Engineering, Tohoku University, Sendai 980-8579, Japan. Lilong@ecei.tohoku.ac.jp
[2] School of Electronic Engineering, Xidian University, Xi'an 710071, China

1. Introduction

Mushroom-like electromagnetic band-gap (EBG) structures exhibit two kinds of bands characteristics: one for surface wave suppression and the other for in-phase reflection. The locally resonant behavior provides a high impedance reflectivity and prevents the propagation of radio-frequency surface currents along the structure. The feature of surface-wave suppression helps to improve integrated circuits and antenna performance such as increasing the antenna gain, reducing mutual coupling and back radiation. Meanwhile, the in-phase reflection feature leads to an artificial magnetic conductor and low profile antenna designs.

An important question arises: what is the relation between the surface wave suppression band gap and the plane wave in-phase reflection frequency band? Recently, some discussions about the fundamental electromagnetic properties and corresponding relations of two bands were put forward [1]-[6]. It has been shown that the relation between the surface wave bandgap and the plane wave in-phase reflection band is very complex and inconclusive up to now. In this paper, we report the rigorous numerical simulations and experimental results of properties and relations of two bands. The primary differences between the present work and the previous investigations are (a) the characteristics of two bands are independently investigated by using the same full-wave analysis models, (b) the corresponding effects of each parameter on the two bands are given to analyze the complex relations, (c) the design guidelines for EBG structures simultaneously taking on in-phase reflection and surface wave bandgap in a certain frequency band are given.

2. Two Bands Characteristics of Mushroom-Like EBG Structures

The mushroom-like EBG structure, as shown in Fig. 1, consists of an array of square metal patches on a flat metal sheet. They are arranged in a two-dimension square lattice and connected to ground by vertical metal plated vias. The surface wave bandgap and the reflection phase of mushroom-like EBG structure are mainly determined by five parameters: patch width (W), gap width (g), substrate permittivity (ε_r) and thickness (t), and vias radius (r). a is the period of the EBG structure ($a=W+g$). The infinite periodic model, i.e., a single cell of EBG structure with periodic boundary conditions (PBC) on four sides, is used to analyze the effects of EBG structure parameters one by one upon the two bands independently. The EBG structure illustrated has the following starting design parameters:

$$W = 0.14\lambda_{6GHz},\ g = 0.006\lambda_{6GHz},\ t = 0.03\lambda_{6GHz}, r = 0.01\lambda_{6GHz},\ \varepsilon_r = 2.65 \quad (1)$$

where λ_{6GHz} is the free space wavelength at 6.0GHz, which is used as a reference length to define the physical dimensions of various EBG structures studied in this paper. Figure 2(a) shows $k-\beta$ dispersion diagram simulation of surface modes propagating in the EBG structure. Calculation inside this special Brillouin zone will provide sufficient knowledge on the surface wave bandgap.

The reflection phase is defined as the phase of reflected electric field at the observational plane, which is normalized to the phase of incident electric field at the same plane. The reflection phase of the EBG structure varies continuously from 180° to -180° versus frequency, which can satisfy PMC-like condition in a certain frequency band. The same full-wave analysis model as the surface wave band-gap analysis is established to evaluate the reflection phase of plane wave normal incidence on the EBG surface, as shown in Fig. 2(b).

ISBN: 978-4-88552-223-9 C3055©IEICE

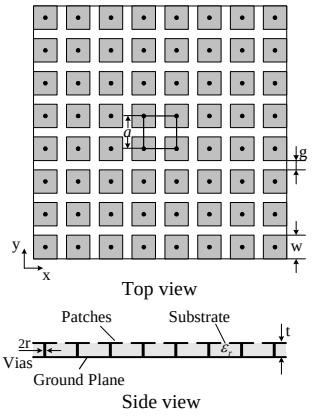

(a)

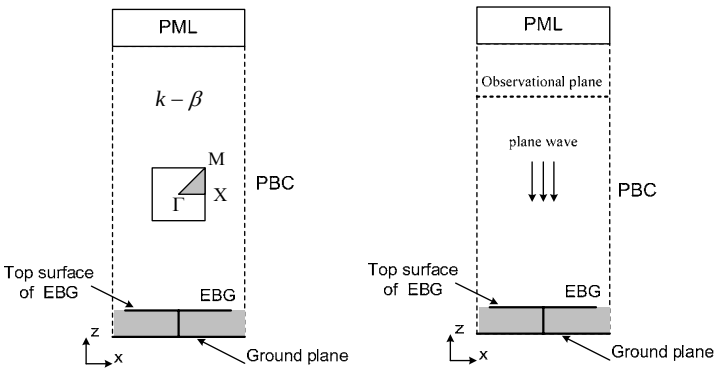

(b)

Figure 1: Geometry of a mushroom-like EBG structure. Figure 2: Infinite periodic models based on the finite element algorithm for (a) calculating the dispersion diagram in the irreducible Brillouin zone and (b) calculating the reflection phase of a plane wave normal incidence, in which the periodic boundary conditions (PBC) are put around the EBG cell to model an infinite EBG surface.

Figure 3(a) shows the numerically simulated $k-\beta$ dispersion diagram of the surface modes propagating in the EBG structure, which was conducted by HFSS based on finite-element method full-wave analysis [7] using the computational model shown in Fig. 2(a). We can observe a complete stopband between the first mode TM_0 and the second mode TE_1 in the frequency band 5.771-8.45GHz. In this figure, Γ, X and M stand for symmetric points in the irreducible Brillouin zone. Figure 3(b) shows the frequency response of transmission coefficient S21, both TM and TE surface waves measured by using a pair of small monopole antennas oriented normally (TM mode) and parallel (TE mode) to the EBG surface. It can be seen that the simulated surface wave bandgap is in good agreement with the measured result. In Fig. 3(b) we also present the measured reflection phase points corresponding to the surface wave suppression band edges of the same EBG structure for normal incidence. It can be seen that the surface wave suppression band edges correspond to the 146.5^o and -89.1^o phase points. The $\pm 90^0$ reflection phase points are also noted.

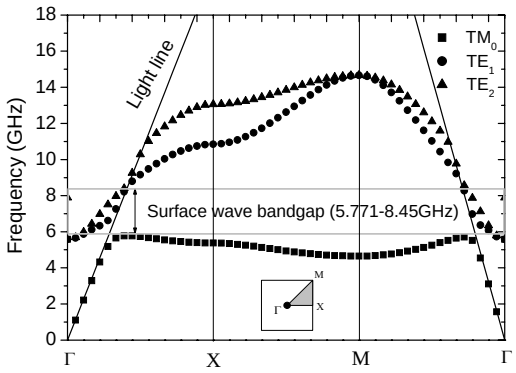

(a)

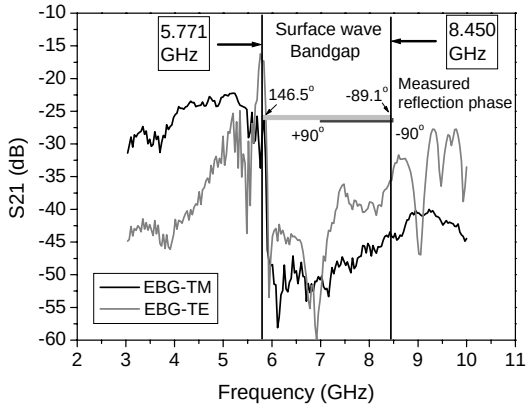

(b)

Figure 3: Measurement and simulation of surface wave bandgap of the EBG structure. (a) Simulated surface wave band structure. (b) Measured TM and TE surface waves transmission coefficients and reflection phase points corresponding to the surface wave band edges for the EBG structure.

The corresponding states of each parameter effect on the surface wave suppression bandgap and in-phase reflection band are given to clarify the arguments about the complex relations. Figure 4(a)-(e) show the surface wave bandgap and the reflection phase of a plane wave normally illuminating the EBG surfaces with different patch widths, gap widths, substrate thicknesses, permittivities, and vias radii, respectively. It is worthwhile to point out when each parameter is changed, other parameters are kept the same as in (1). The frequency range between two circles in each curve represents the position of the surface wave suppression bandgap of the EBG structure, which is calculated by the

simulation of dispersion diagram. The electromagnetic characteristics of and the relations between the two bands can be obtained from these results.

1) The surface wave bandgap for TM and TE modes is not necessarily related to the in-phase reflection band. But the variations of the two bands with EBG parameters are almost the same, that is, we can predict the effects of EBG parameters on the position and the bandwidth of the surface wave suppression bandgap by using their effects on the position and the slope of the in-phase reflection band.

2) The metal vias play an important role in determining the surface wave suppression bandgap. There is no bandgap of the surface wave suppression in the structure without vias, nevertheless, the in-phase reflection band still exists. It can be observed that the reflection phase characteristics are nearly unchanged when the vias radius is much less than the patch width ($W/r > 14.0$ in this example). But when the vias radius is increased, the reflection phase band will increase and its bandwidth will decrease, which is due to the coupling between the metal vias and the gap of adjacent patches. Moreover, the edge of the TM surface wave band gradually approaches the frequency point of $+90^\circ$ reflection phase with the increase of vias radius.

3) The correspondence of the two bands can be effectively adjusted by the parametric ratio of period to thickness *a*/*t* (assume *r* is kept smaller). Numerical tests show that, when $a/t < 2.0$, the surface wave bandgap lies between the $\pm 90^\circ$ reflection phase frequencies for normal incidence. In practice, it is highly desirable to find a material that simultaneously shows the in-phase reflection and the surface wave bandgap in a certain frequency band.

It is known that even if *t* is small as compared to the wavelength but large as compared to *a*, one can consider the interaction between the metal patch and the ground plane as the far-zone, i.e., only the fundamental-mode plane wave between array and the ground. It leads to transmission-line formula for the equivalent impedance of the EBG structure. However, if *t* becomes smaller than *a*, one should take into account the influence of higher-order Floquet modes reflected by the ground plane. The influence factor of the evanescent modes can be simply expressed as follows [5]

$$\gamma = \frac{2a}{\lambda}\log\left(1 - e^{-\frac{4\pi t}{a}}\right) < 0, \quad (a << \lambda) \tag{2}$$

It can be seen that the higher-order modes influence turns out to be negligible if $t \approx a/2$, which is consistent with our numerical results. Our results show the previous investigations [1]-[6] are reconcilable, and their primary differences are due to the different corresponding relations of two bands region of mushroom-like EBG structures. When the ratio *a*/*t* increases (>2), the band edge of TM surface wave will gradually deviate the $+90^\circ$ reflection phase frequency and go into the out-of-phase region, as shown in Fig. 4(a) and (d).

4) The relative permittivity of the substrate used to fabricate the EBG structure plays a less important role in adjusting the correspondence of the two bands, as shown in Fig. 4(c).

3. Conclusion

This paper presents a detailed study of the surface wave suppression bandgap and the plane wave reflection phase characteristics of mushroom-like EBG structures. It is revealed that the surface wave bandgap for TM and TE modes is not necessarily corresponding to the plane wave in-phase reflection band. The corresponding relation of two bands is diverse with the parameter variations. But the effects of EBG parameter variations on the two bands characteristics are consistent. Two parametric ratios a/t and W/r play an important role in adjusting the simultaneous appearance of the surface wave suppression bandgap and the plane wave in-phase reflection band in a certain frequency band. Numerical tests show that, when $a/t < 2.0$, the surface wave bandgap generally lies between the $\pm 90^\circ$ reflection phase frequencies for normal plane waves.

Acknowledgments

This work is partially supported by the National Natural Science Foundation of China under contract No. 60601028, and partially supported by JSPS Postdoctoral Fellowship of Japan.

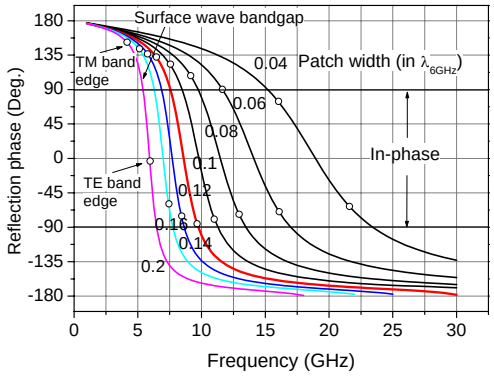

(a)

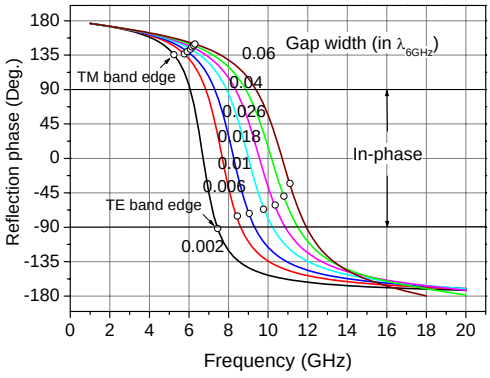

(b)

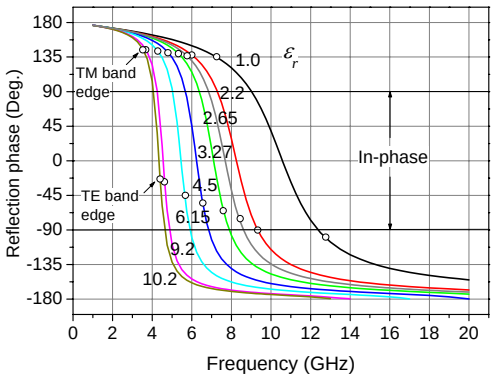

(c)

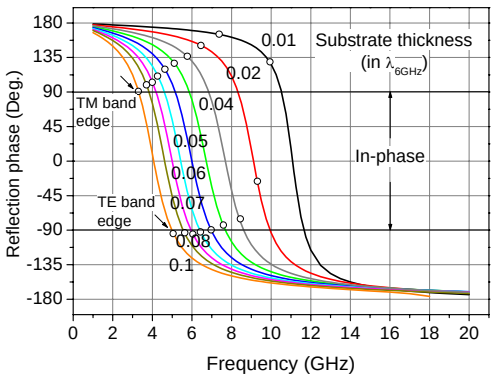

(d)

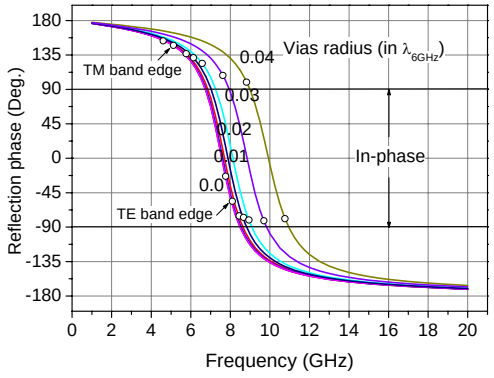

(e)

Figure 4: EBG parameters analysis and corresponding states of two bands. (a) Patch width effect. (b) Gap width effect. (c) Permittivity effect. (d) Substrate thickness effect. (e) Vias radius effect. Note that the frequency region between two circles in each curve represents the position of the surface wave suppression bandgap of the EBG structure.

References

[1] D. Sievenpiper, L. J. Zhang, R. F. J. Broas, N. G. Alexopolus, and E. Yablonovitch, "High-impedance electromagnetic surfaces with a forbidden frequency band," *IEEE Trans. Microwave Theory Tech.*, vol. 47, no. 11, pp. 2059-2074, Nov. 1999.

[2] R. E. Diaz, J. T. Aberle, and W. E. Mckinzie, "TM mode analysis of a Sievenpiper high-impedance reactive surface," *2000 IEEE AP-S Int. Symp. Dig.*, vol. 1, pp. 327-330, July 2000.

[3] F. Yang and Y. Rahmat-Samii, "Reflection phase characterizations of the EBG ground plane for low profile wire antenna applications," *IEEE Trans. Antennas Propagat.*, vol. 51, no. 10, pp. 2691-2703, Oct. 2003.

[4] S. Clavijo, R. E. Diaz, and W. E. Mckinzie, "Design methodology for Sievenpiper high-impedance surfaces: An artificial magnetic conductor for positive gain electrically small antennas," *IEEE Trans. Antennas Propagat.*, vol. 51, no.10, pp. 2678-2684, Oct. 2003.

[5] S. A. Tretyakov and C. R. Simovski, "Dynamic model of artificial reactive impedance surfaces," *J. Electromagn. Waves Appl.*, vol. 17, no. 1, pp. 131-145, 2003.

[6] A. Aminian, F. Yang, and Y. Rahmat-Samii, "In-phase reflection and EM wave suppression characteristics of electromagnetic band gap ground planes," *2003 IEEE AP-S Int. Symp. Dig.*, vol. 4, pp. 430-433, June 2003.

[7] R. Remski, "Analysis of PBG surfaces using Ansoft HFSS," *Microwave J.*, vol. 43, no. 9, pp. 190-198, Sept. 2000.